Experiments on the mechanical behavior of anodically bonded interlayer of Pyrex Glass/Al/Si

Yu-Qun Hu[1,*], Ya-Pu Zhao[2]

[1] College of Civil Aviation and Flight, Nanjing University of Aeronautics and Astronautics, Nanjing 210016, China
[2] State Key Laboratory of Nonlinear Mechanics (LNM), Institute of Mechanics, Chinese Academy of Sciences, Beijing 100190, China
* Corresponding author: hyq@nuaa.edu.cn

Abstract The MEMS/NEMS devices present an attractive prospect in many areas, especially in aviation and aerospace. Anodic bonding is one of the key technologies for the manufacturing of integrated 3-D structures of these devices. In this paper, based on experiments and detailed analysis, a systematic study will be made in depth for the mechanical behavior of anodically bonded interlayer within micro-scale structures. In accordance with a typical anodically bonded structure from one kind of MEMS micro accelerometer, a series of anodic bonding and mechanical tests were completed, for the behavior of the interlayer under quasi-static loading. The paper also presents the analysis of some important factors which influence the mechanical properties of the anodically bonded structure of Pyrex 7740 Glass/Al/Si. The metal oxidation reaction, dendritic nanostructures, and fractal patterns, which taking place at the bonding interface, were scrutinized. The experimental results demonstrate the thickness effect of the intermediate layer, and that the bonding tensile strength increases with the bonding temperature and voltage, but it decreases with the increase of the thickness of Al intermediate layer. The formation of the nanostructures in the bonding interlayer is also helpful to enhance the anodic bonding strength.

Keywords Anodic bonding, MEMS/NEMS, Intermediate layer,

1. Introduction

Three-dimensional (3-D) integration technologies related to Micro/Nano Electro-Mechanical Systems (MEMS/NEMS) devices is becoming one of focused research areas[1-5]. Anodic bonding is one of the key technologies for the manufacturing of integrated 3-D structures of these devices. In MEMS/NEMS devices, anodic bonding technology, especially for the connection of multilayer materials, offers a great prospect to extend the structural integration of the devices from two-dimensional (2-D) to 3-D, as shown in Figure 1. 3-D integration based on anodic bonding offers the potential for high performance and high-density applications due to lower power consumption, enhanced transmission speeds, better performance, and smaller device size[6].

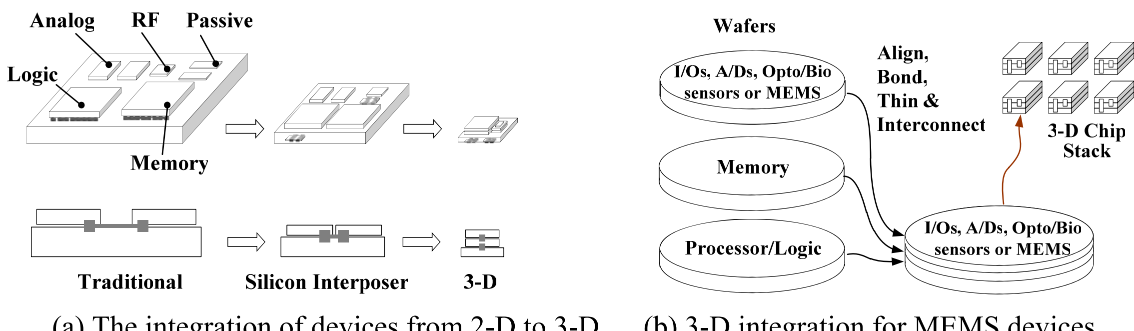

(a) The integration of devices from 2-D to 3-D (b) 3-D integration for MEMS devices

Figure 1. The trend for the integration of MEMS/NEMS devices (revised from reference [1])

Anodic bonding, also known as electrostatic bonding or field-assisted bonding, was developed as a means to connect metals, alloys or semiconductors to conductive glasses. It is also a highly

promising method for joining certain metals or semiconductors to alkali-ion-conductive glasses at decreased temperatures. Compared to other techniques, the main advantage of anodic bonding is that a strong junction interface can be achieved at a reduced bonding temperature by application of an electric field [7-9]. The temperature for anodic bonding is usually lower than the softening point of glass and the melting points of the materials selected for this purpose. Nowadays, there exists a demand for this straightforward and reliable bonding technique in connecting, packaging, or hermetic sealing of more complex micro/nano structures and integrated microcircuits in MEMS/NEMS devices. The promising applications of MEMS devices are still limited by the reliability of MEMS devices, especially in the applications for military and aerospace systems.

Some previous studies [10, 11] show that one of the important structural failure mode is the stripping of micro anchors from its substrate in some type of MEMS devices. On the basis of the structure of these devices, in this paper, we report some mechanical tests on the micro anchors anodically bonded between Pyrex 7740 glass wafer and aluminum thin film coated on crystalline Si wafer.

2. Experimental

2.1. Specimen preparation

The experimental specimens were made by die-level anodic bonding at different temperatures and voltages. The mesa structures are used to avoid the edge micro cracks due to the chip dicing process. Pyrex 7740 glass wafers of 500 μm thickness and 100 mm diameter were cut into 12 mm ×12 mm square chips. The chemical composition of Pyrex 7740 wafer includes 80.8 Mol% SiO_2, 12.0 Mol% B_2O_3, 4.2 Mol% Na_2O, 2.0 Mol% Al_2O_3, 0.6 Mol% K_2O, 0.2 Mol% MgO, and 0.2 Mol% CaO, as shown in Table 1 [12].

Table 1. Chemical composition of Pyrex 7740 glass wafer (Mol%)

SiO_2	B_2O_3	Na_2O	Al_2O_3	K_2O	MgO	CaO
80.8 %	12.0 %	4.2 %	2.0 %	0.6 %	0.2 %	0.2 %

Si wafers were of 100 mm in diameter (double-side polished, p-type, and wafer surface plane (100), and were patterned into mesas with different-sized squares. There are four types of dice with different mesa spacing, as shown in Figure 2. These mesas were of 10 μm in height and were prepared with a deep reactive ion etch (DRIE) process. These patterned Si wafers were coated by an ARC-12M sputtering system with pure aluminum (99.999%). The coated aluminum thin films were of 500 Å, 950 Å, 1500 Å, and 2300 Å in thicknesses respectively. Then these Si wafers were also diced into squares of 12 mm ×12 mm. All square samples were cleaned by deionized water spray rinse in a 100-class clean room and dried by nitrogen gas under pressure.

A pair of glass chip and well-coated crystalline silicon chip was placed between two stainless steel plates, which acted as plate electrodes, and then between two hot plates. The glass side was connected with the cathode, and the silicon side was connected with anode. The schematic of this bonding configuration is shown in Figure 3.

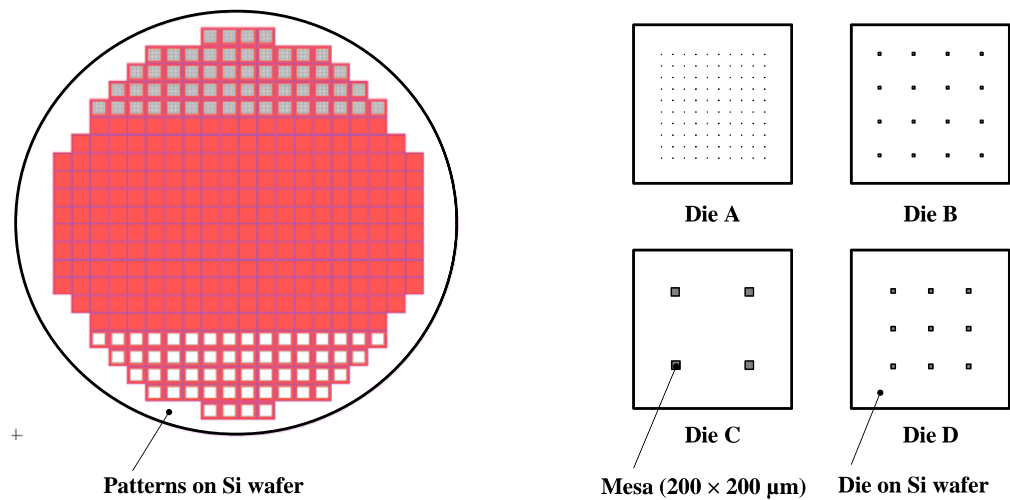

Figure 2. The Silicon wafer patterned with dice

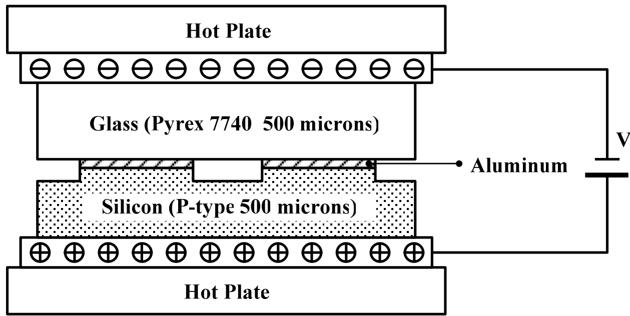

Figure 3. The schematic of specimen bonding configuration

The anodic bonding of these specimens was performed at the temperature range from 300°C to 375°C and at the voltage range from 150V to 500V for less than 30 minutes on an open (non-vacuum) bonding system. The bonding voltage was applied after the selected bonding temperature was reached. When the bonding was completed, the bonded sample was cooled to room temperature in 2 hours.

Before the upcoming tests, all specimens were examined under optical microscope. Some of the glasses were removed to expose the aluminum film for the SEM microanalysis with energy dispersive X-ray (EDX) and EBSD. The specimens were examined in a Sirion 400NC (FEI Field Emission Gun SEM) with the EBSD system (INCA Energy and Crystal System of Oxford).

2.2. Transmission electron microscopy

To prepare TEM test, the bonded samples were cut into small bars with a cross-section of 1.5mm×1.5mm (perpendicular to the interface). These small bars were individually glued into 3mm diameter copper tubes with an inner diameter of 2.2 mm. After the glue was cured on the Nuova II curing stage, these copper tubes were sectioned into slices approximately 750 μm thick, and then ground down to a thickness of about 40 μm and dimpled at the interface. Before argon-ion milling, these foils were attached to molybdenum support rings with an inner diameter of 1 mm. Specimens

were ion milled to electron transparency at room temperature by a Gatan Model 691 precision ion polishing system (PIPS). All TEM specimens were examined in a 300 kV Tecnai F30 (FEI Field Emission Gun TEM with LaB6 filament). STEM and energy dispersive X-ray (EDX) spectroscopy microanalysis were used for chemical analysis.

2.3. Tensile experiment under quasi-static loading

In order to characterize the bonding strength, each bonded chip was diced into 4 mm × 4 mm specimens by an automated dicing saw. Before the tensile test, all samples for tensile tests were examined under an optical microscope with 50× objective lens to exclude defective ones. The specimens were attached to aluminum jigs with glue for the tensile test. The bonding strength was measured by a tensile pulling machine (GATAN Microtest 2000) and the specimen under test was pulled perpendicular to the bonding interface until its rupture. The test pulling speed was 1 mm/min, and the pulling speed and the data acquisition were controlled by a personal computer. In these pulling tests, it was found that the maximum failure loads of these specimens were less than 5 N, and the specimens were easily damaged when they were fixed to rigid fixtures of the test machine. The alignment of the test studs is of critical importance because small deviations will induce bending moments which can cause premature failure of the test sample [13]. To improve the alignment of test samples and to avoid the early failure caused by the force from sample installation, a special fixture was designed with flexible steel wire strand, as shown in Figure 4.

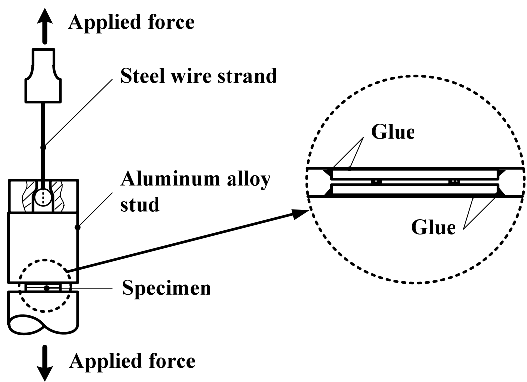

Figure 4. Schematic of fixture for tensile tests

3. Results and discussion

3.1. Fractures in bonded specimens

When all the bonding specimens were examined under optical microscope, fractures were found in some of the specimens, as indicated by white arrows in Figure 5. The fractures occurred in the glass side at the corner of the mesas, and many of them were found in the samples anodically bonded at higher bonding temperature. During the process of anodic bonding, when the bonding temperature was larger than 350°C, the fractures of this type were easily found in some specimens. This kind of fractures seldom occurred in the specimens bonded at the temperature of no more than 350°C. The reason for the occurrence of these fractures is the different thermal expansion coefficient with Pyrex

7740 glass and silicon. The higher the bonding temperature was, the larger the difference of thermal expansion coefficient between the glass and silicon, that is, the larger the residual stress was. The residual stress results in these fractures.

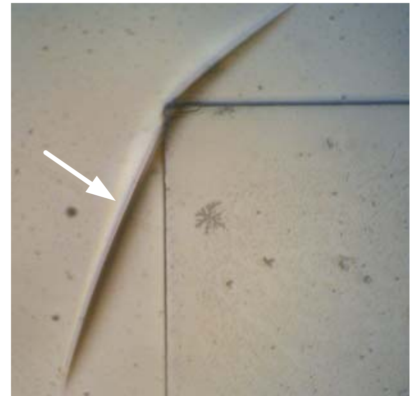

(a) Bonding temperature at 350 °C

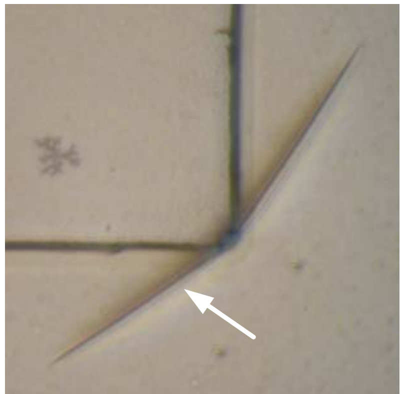

(b) Bonding temperature at 375 °C

Figure 5. The typical fractures in the samples with Al film of 950 Å

3.2. Fractal patterns and dendritic nanostructures

3.2.1. Fractal patterns

With the optical microscope, many fractal patterns were found in the intermediate aluminum film, as shown in Figure 6. The size of the patterns decreases with the thickness of Al film and increases with the bonding temperature. The fractal patterns in the aluminum film have the characteristics of two-dimensional Diffusion-Limited Aggregation (DLA) model [14, 15]. The fractal dimensions of the typical fractal patterns are calculated by sand-box method [16, 17].

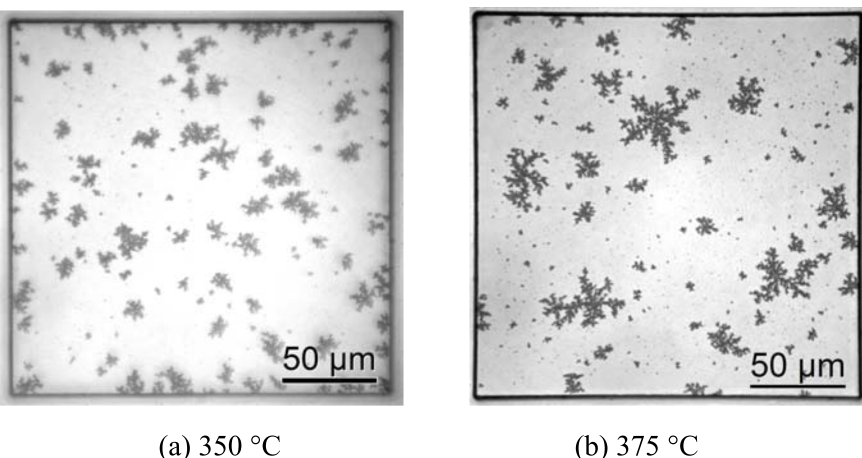

(a) 350 °C (b) 375 °C

Figure 6. Fractal patterns distribution in 500 Å thick Al film at different bonding temperatures

The fractal patterns in the intermediate aluminum film have the typical dimension of 2-D DLA process, and their fractal dimension is around 1.7, as listed in Some fractal patterns were analyzed with the EDX and EBSD systems of INCA. The microanalyses show that the fractal patterns contain the crystalline grains of Aluminum and Silicon. These fractal patterns were formed in the process of anodic bonding due to the limited diffusion and aggregation of Si atoms in the Al film.

These diffused Si atoms mainly originate from the following chemical reaction, $4Al + 3SiO_2 = 2Al_2O_3 + 3Si$. When the temperature is above 300°C, there exists a chemical reaction between the Al and SiO_2 [18]. The silicon dioxides come from the slightly oxidizing of silicon wafer on its exposed surface before the aluminum sputtering process of these silicon wafers.
Table 2.
Some fractal patterns were analyzed with the EDX and EBSD systems of INCA. The microanalyses show that the fractal patterns contain the crystalline grains of Aluminum and Silicon. These fractal patterns were formed in the process of anodic bonding due to the limited diffusion and aggregation of Si atoms in the Al film. These diffused Si atoms mainly originate from the following chemical reaction, $4Al + 3SiO_2 = 2Al_2O_3 + 3Si$. When the temperature is above 300°C, there exists a chemical reaction between the Al and SiO_2 [18]. The silicon dioxides come from the slightly oxidizing of silicon wafer on its exposed surface before the aluminum sputtering process of these silicon wafers.

Table 2. The typical fractal dimensions of the fractal patterns in the Al films[19]

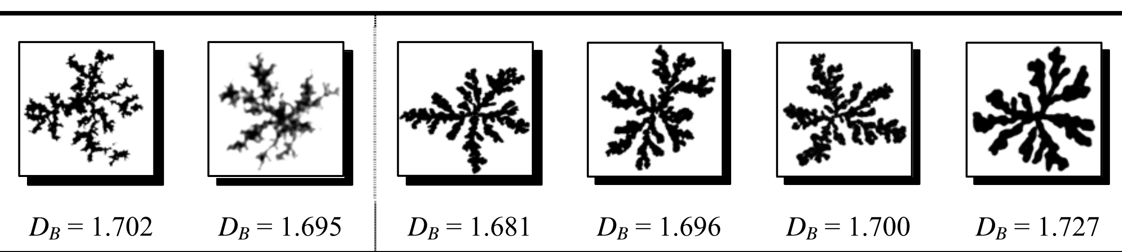

D_B = 1.702	D_B = 1.695	D_B = 1.681	D_B = 1.696	D_B = 1.700	D_B = 1.727

When the Al film is thin enough, the fractal patterns run through the span of the whole thickness of the film, and bond with the substrate and glass. The strength of chemical bond is 799.6±13.4 kcal/mol for Si-O, 511±3 kcal/mol for Al-O, and 325±7 kcal/mol for Si-Si [20]. Therefore, the fractal pattern improves the bonding strength between the Pyrex glass and the aluminum thin film coated on the silicon substrate.

3.2.2. Dendritic nanostructures

In all anodically-bonded samples, dendritic nanostructures were found in the Pyrex glass near the Al/glass interface, as shown in Figure 7. The dendritic nanostructures, which are seen over the whole thin area, exhibit a similar maximum height of 600-650 nm in the specimens bonded at 350°C, 400 V. These three-dimensional treelike structures have a trunk of tens nanometers in diameter (less than 40 nm). TEM cannot show all the small branches of these 3-D dendritic nanostructures.

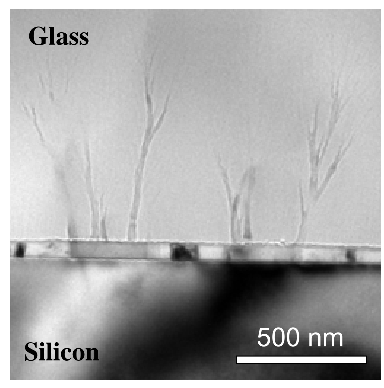

(a) 50 nm aluminum film

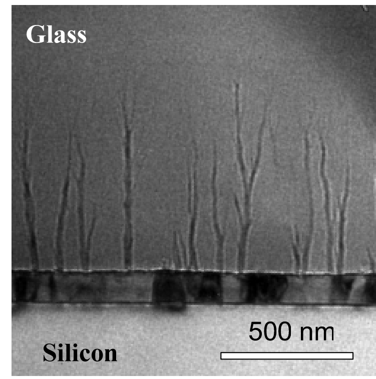

(b) 95 nm aluminum film

Figure 7. Dendritic nanostructures of specimens at 350°C and 400 V

Figure 8 illustrates the EDX analysis position and element analysis result of the nano dendritic structures under STEM mode. The electron beam scanning path is marked with a black thick line across three trunks of the dendritic structures, as shown in Figure 8(a). Element analysis indicates that the dendritic nanostructures are aluminum enriched, as shown in Figure 8(b). STEM/EDX microanalysis provides enough evidence of diffusion of aluminum into the Pyrex glass during anodic bonding. Examined by EDX, the trunks exhibit lesser counts of silicon and oxygen while the aluminum counts are conspicuously increased.

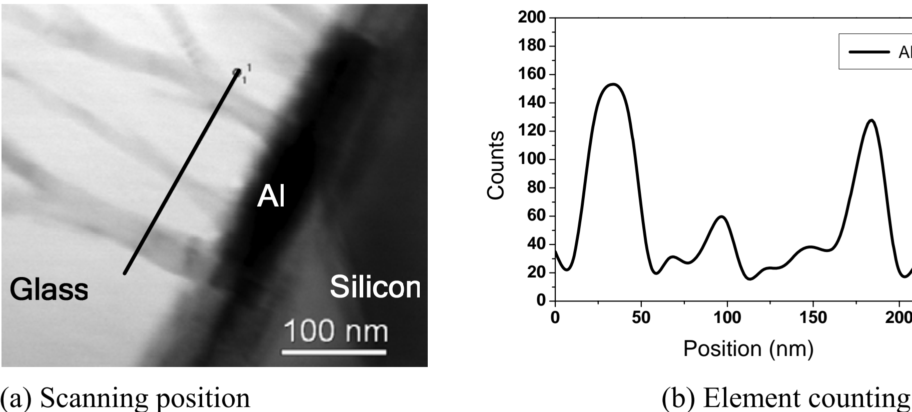

(a) Scanning position (b) Element counting

Figure 8. Scanning position and element counting for EDX analysis

3.2. Bonding strength

The mean bonding tensile strength are shown in Figure 9. Bonding tensile strength, which is averaged from the results of five or more specimens. The measured bonding strength values exhibit a rather large variance around a mean value. This can be attributed to several aspects, such as the misalignment of specimens, the characteristics of bonding behavior [21], the micro defects due to residual stress, and etc. All the specimens pulled apart were also examined with the optical microscope and scanning electron microscope (SEM), and some parts of the aluminum film and the Pyrex glass were residual on the opposite side.

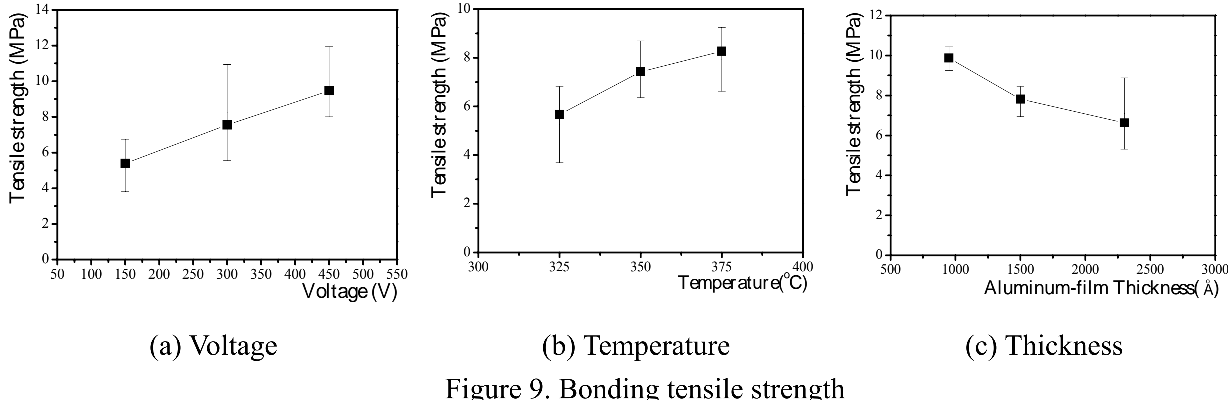

(a) Voltage (b) Temperature (c) Thickness

Figure 9. Bonding tensile strength

Figure 9(a) shows the tensile strength increases with the bonding voltage ranged from 150 to 450 V. The specimens in Figure 9(a) were bonded with 700 µm thick Pyrex 7740 glass wafer at 300°C, and their aluminum film is 1300 Å thick. In the process of anodic bonding, the higher bonding voltage means the larger force produced by the electrostatic field across the bonding interface, and brings about much larger and more intimate contact area between the bonding pairs, that is, more chemical bonds generated at the bonding interface and an enhancement of the bonding strength. On the other hand, the higher the bonding voltage is, the more amounts of movable ions will be produced in the glass and then the more anions, mainly O^{2-}, will accumulate in the bonding glass adjacent to the interface of glass/Al, which provides more opportunities to form the chemical bonds between oxygen and aluminum. Unfortunately, a high bonding voltage will introduce a risk of electric breakdown, and the maximum bonding voltage is limited mainly by the breakdown voltage over the depleted layer.

The tensile test results tell that the maximum failure loads also increases with the bonding temperature from 325 to 375°C, as shown in Figure 9(b). The specimens used in Figure 9(b) were bonded with 500 µm thick Pyrex 7740 glass wafer, and the thickness of aluminum film is 500 Å. Pyrex 7740 glass has a complicated chemical composition and contains some important alkali elements, which are responsible for the ionic current in the glass during the anodic bonding process. The increasing of bonding temperature gives rise to more amounts of the cations, and correspondingly induces a large number of anions to accumulate near the bonding interface, which also provides more opportunities to produce chemical bonds with aluminum in anode and then improves the bonding strength. But a high bonding temperature not only will lead to the degradation of metal leads and integrated circuits in MEMS device, but also will induce large thermal stress. In the high temperature bonding tests, cracks were found in the glass of some specimens due to thermal stress, as shown in Figure 5.

When comparing the tensile failure loads from the specimens which were bonded under the same temperature, voltage, and duration time but with the different thicknesses of aluminum film, we find that their bonding tensile strength increases with the decrease of aluminum film thickness in our tested range, as shown in Figure 9(c). All the tested samples in Figure 9(c) were anodically bonded under 300°C and 400 V. The mean tensile strength increases from 6.6 to 9.9 MPa, while the Al film thickness decreases from 2300 to 950 Å, which indicate a fact that the experimental results show the remarkable size effect. The bonding strength is affected by the thickness of Al film within the tested range of Al thickness.

4. Summary

In summary, the tensile specimens were anodically bonded at the relatively low temperature and voltage, using Pyrex 7740 glass and patterned crystalline silicon chips coated with Al film. To investigate the mechanical behavior of anodically bonded interlayer of Pyrex Glass/Al/Si, the tensile experiments were completed with the newly designed flexible fixtures, and the analysis for the anodically bonded intermediate layer were also made with SEM and TEM.

The formation of the fractal patterns in the process of anodic bonding is due to the limited diffusion, aggregation, and crystallization of Si and Al atoms in the intermediate Al film. These fractal patterns have the fractal dimension of 2-D DLA process, and their fractal dimension is around 1.7.

These fractal patterns in the intermediate Al film consist of Al and Si crystalline grains.The fractal patterns improves the bonding strength between the Pyrex 7740 glass and the Al intermediate layer coated on the crystal silicon substrate.

The formation of the dendritic nanostructures is due to the diffusion and reaction near the glass/Al interface under a non-equilibrium condition during the anodic bonding process. These nanostructures might reveal helpful clues in improving the bonding quality. The dendritic nano-crystalline structures are shown to be one of the key structures for the improvement of strength in anodic bonding.

Test results demonstrated that, the bonding strength increases with the bonding temperature and voltage. This is in agreement with earlier results reported in the literature. But the experiments exhibit that the tensile strength decreases with the increase of the thickness of Al intermediate layer. Although the measured bonding strength values exhibit a rather large variance around a mean value, the experimental results can be referenced qualitatively. With the dimensions of MEMS devices downward, the scale effect in anodically bonded micro anchors should be considerable during the process of device design.

Acknowledgements

We would like to thank Mr. Wan Lap Yeung of Hong Kong University of Science and Technology and Dr. Jijia Xie and Mr. Chuang Feng for their help during specimen preparation and tensile experiments. This work was supported by the National Natural Science Foundation of China (NSFC) (Grant No. 11272144) and the Jiangsu Provincial Natural Science Foundation of China (Grant No. BK2011725).

References

[1] S. Farrens. Wafer and Die Bonding Technologies for 3D Integration. In: Materials and Technologies for 3-D Integration. F. Roozeboom, C. Bower, P. Garrou, et al., Ed. Warrendale: Materials Research Society. 2009. pp. 55-65.

[2] M.M. Koebel, N. El Hawi, J. Lu, et al. Anodic bonding of activated tin solder alloys in the liquid state: A novel large-area hermetic glass sealing method. Solar Energy Materials and Solar Cells. 2011, 95 (11), pp.3001-3008.

[3] Z. Wang, D. Wang, N. Jiao, et al. Nanochannel system fabricated by MEMS microfabrication and atomic force microscopy. Iet Nanobiotechnology. 2011, 5 (4), pp.108-113.

[4] M.M.V. Taklo, N. Lietaer, H.R. Tofteberg, et al. 3D MEMS and IC integration. In: Materials and Technologies for 3-D Integration. F. Roozeboom, C. Bower, P. Garrou, et al., Ed. Warrendale: Materials Research Society. 2009. pp. 211-220.

[5] F. Niklaus, J.-Q. Lu, J.J. McMahon, et al. Wafer-level 3D integration technology platforms for ICs and MEMs. In: Proceedings of the twenty second international vlsi multilevel interconnect conference (VMIC), IMIC. 2005.

[6] J.H. Lau. Recent advances and new trends in nanotechnology and 3D integration for semiconductor industry. 2011 IEEE International 3D Systems Integration Conference (3DIC). 2012, pp.23 pp.-23 pp.

[7] G. Wallis, D.I. Pomerantz. Field Assisted Glass-Metal Sealing. Journal of Applied Physics. 1969, 40 (10), pp.3946-3949.

[8] Q. Xing, G. Sasaki, H. Fukunaga. Interfacial microstructure of anodic-bonded Al/glass. Journal of Materials Science: Materials in Electronics. 2002, 13 (2), pp.83-88.

[9] J. van Elp, P.T.M. Giesen, J.J. van der Velde. Anodic bonding using the low expansion glass ceramic Zerodur. Journal of Vacuum Science and Technology B. 2005, 23 (1), pp.96-98.

[10] L.S. Wang, Y.Q. Hu, Z. Hong, et al. Failure Analysis of Micro-accelerometer under Impact Loading. Journal of Mechanical Strength. 2001, 23 (4), pp.516-522.

[11] Y.Q. Hu, L.S. Wang, Z.J. Zeng, et al. Structural Failure Analysis and Numerical Simulation of Micro-accelerometers under Impulsive Loading. International Journal of Nonlinear Sciences and Numerical Simulation. 2002, 3 (NOS.3-4), pp.311-314.

[12] J.E. Shelby. Effect of radiation on the physical properties of borosilicate glasses. Journal of Applied Physics. 1980, 51 (5), pp.2561-2565.

[13] A. Plößl, G. Kräuter. Wafer direct bonding: tailoring adhesion between brittle materials. Materials Science & Engineering R-Reports. 1999, R25, pp.1-88.

[14] T.A. Witten, L.M. Sander. Diffusion-limited aggregation. Physical Review B. 1983, 27 (9), pp.5686-5697.

[15] T.A. Witten Jr, L.M. Sander. Diffusion-Limited Aggregation, a Kinetic Critical Phenomenon. Physical Review Letters. 1981, 47 (19), pp.1400-1403.

[16] S.R. Forrest, T.A. Witten. Long-range correlations in smoke-particle aggregates. Journal of Physics. A. 1979, 12 (5), pp.L109-L117.

[17] S.W. Russell, J. Li, J.W. Mayer. In situ observation of fractal growth during a-Si crystallization in a Cu3Si matrix. Journal of Applied Physics. 1991, 70 (9), pp.5153-5155.

[18] N.J. Chou, J.M. Eldridge. Effects of material and processing parameters on the dielectric strength of thermally grown SiO_2 films. Journal of the Electrochemical Society. 1970, 117 (10), pp.1287-1293.

[19] Y.Q. Hu, Y.P. Zhao, T.X. Yu. Fractal Pattern Formation in Anodic Bonding of Pyrex Glass/Al/Si. International Journal of Nonlinear Sciences and Numerical Simulation. 2008, 9 (4), pp.315-322.

[20] D.R. Lide. Handbook of Chemistry and Physics. Boca Raton, FL: CRC Press. 2005.

[21] B. Müller, A. Stoffel. Tensile strength characterization of low-temperature fusion-bonded silicon wafers. Journal of Micromechanics and Microengineering. 1991, 1 (3), pp.161-166.